

---

# GEOHERMAL ASSESSMENT AND MODELING OF THE UINTA BASIN, UTAH

*Christian L. Hardwick<sup>1\*</sup>, Hobie W. Willis<sup>1</sup>, and Mark L. Gwynn<sup>1</sup>*

---

## ABSTRACT

Co-produced waters from sedimentary basins may represent a significant geothermal resource. This study presents a regional assessment of the geothermal potential for co-produced waters from oil and gas fields of the Uinta Basin in northeastern Utah using bottom-hole temperature (BHT) and co-produced water data for 776 oil and gas wells along with available lithological information. For 136 of the wells, a BHT correction is applied using Horner and single-BHT correction methods to account for drilling-induced temperature field disturbances. A conservative depth-dependent correction of +2.0°C/km (+0.11°F/100 ft) was derived from 50 Uinta Basin wells with reliable Horner corrections and is applied to BHTs with insufficient data for other correction methods. Corrected temperatures and typical thermal conductivities are used to calculate thermal gradients and surface heat-flow values for each well. Calculations reveal an average geothermal gradient of about 27°C/km (1.48°F/100 ft), implying wells producing from depths greater than 2 km (6562 ft) in the basin will likely have temperatures greater than 65°C (149°F). The average heat-flow value from wells with corrected BHTs is 67 mW/m<sup>2</sup>. These results are generally typical for gradient and heat-flow values in the Colorado Plateau. Thermal outputs are calculated using well production rates and fluid temperatures. The average thermal output is 88 kW per well with a maximum output as high as 10 MW—energy which is currently lost to waste water. The highest output wells are mostly a result of high volumetric production rates and are located in the Ashley Valley field. Thermal models for the basin were created using a 3-dimensional, finite-element modeling program (COMSOL Multiphysics 4.4) and were calibrated to corrected well temperatures. Preliminary models reveal an area of approximately 16,000 km<sup>2</sup> (6180 mi<sup>2</sup>) with temperatures above 75°C (167°F) at 2 km (6560 ft) depth, and an area of 5500 km<sup>2</sup> (2120 mi<sup>2</sup>) with temperatures above 150°C (302°F) at 5 km (16,400 ft) depth. Co-produced water temperatures in 740 wells are above 50°C (122°F) and may be suitable for direct-use applications such as greenhouses, space heating, and aquaculture. Binary geothermal power plants generally require a minimum temperature of 140°C (284°F) to achieve acceptable efficiency and 36 wells (~5%) across the basin meet or exceed such temperatures. The thermal regime and existing infrastructure make the Uinta Basin a candidate for extensive direct-use geothermal applications and possibly binary geothermal power generation.

---

## INTRODUCTION

The thermal regime of a sedimentary basin controls the maturity of hydrocarbon systems within the basin and the overall geothermal energy potential (Luheshi, 1983; Willett and Chapman, 1987; Deming and Chapman, 1988, 1989; Prenskey, 1992; Hermanrud and others, 1990; Förster, 2001; Kutasov and Eppelbaum, 2005; Zschocke, 2005; Goutorbe and others, 2007). This limited, yet robust, study focuses on the geothermal energy potential of fluids co-produced from hydrocarbon plays by examining temperature data and other thermal properties from oil and gas wells in the Uinta Basin (figure 1). The first commercial gas production in the Uinta Basin began in 1925, but further development was limited until 1948 when oil was discovered in the Permian Park City and Phosphoria Formations and in the Pennsylvanian Weber Sandstone (Clem, 1985). Over 15,700 wells have now been drilled across large tracts of the Uinta Basin (U.S. Bureau of Land Management, 2012). Bottom-hole temperatures (BHT) extracted from oil and

gas well logs constitute a majority of the subsurface temperature data throughout the world and this is certainly true of the Uinta Basin. These data are typically readily available, relatively inexpensive, and abundant in many study locations (Förster and Merriam, 1995; Henrikson, 2000; Henrikson and Chapman, 2002; Morgan and Scott, 2014). Aside from sporadic temperatures recorded in relatively shallow water supply wells, BHTs often constitute the only available subsurface temperature data. Heat flow and geothermal energy potential can be calculated from BHTs, associated thermal conductivities, and the consequent thermal gradient inherent in each well (Chapman and others, 1984).

However, there is a major problem with BHT data because the temperature of the surrounding rock is temporarily altered during the drilling process. Although some frictional heat is generated by the drill bit, the predominant effect is cooling that comes from the circulation of relatively cold drilling fluids (Guyod, 1946; Bullard, 1947; Lachenbruch and Brewer, 1959; Dowdle and

---

<sup>1</sup> *Utah Geological Survey  
1594 W. North Temple  
Salt Lake City Utah 84116  
\*phone: (801) 538-5412  
christianhardwick@utah.gov*

Hardwick, C.L., Willis, H.W., and Gwynn, M.L., 2015, Geothermal Assessment and Modeling of the Uinta Basin, Utah, *in* Vanden Berg, M.D., Resselar, R., and Birgenheier, L.P., editors, *Geology of Utah's Uinta Basin and Uinta Mountains*: Utah Geological Association Publication 44, p. 337-353.

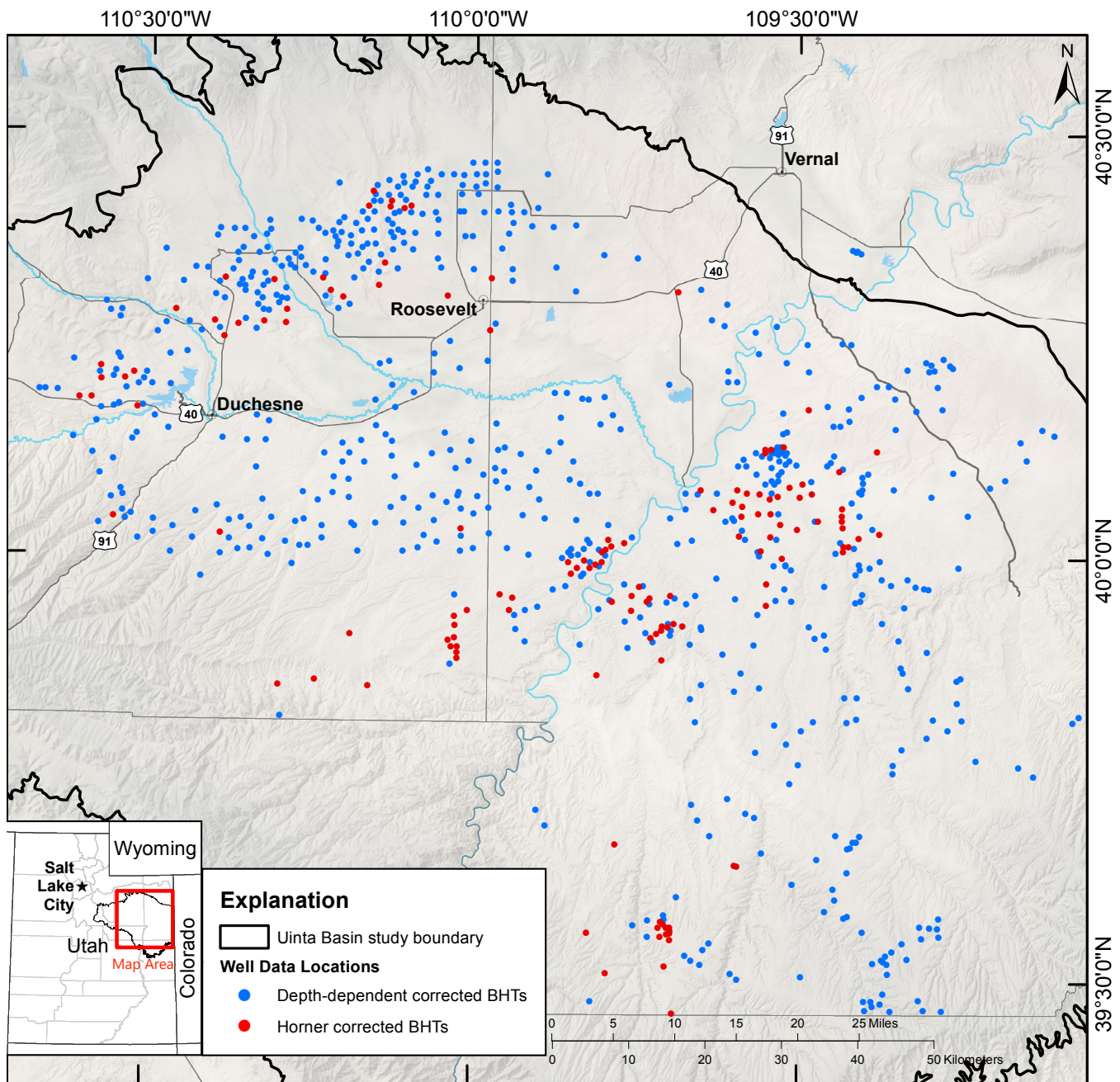


**Figure 1.** Map of Uinta Basin showing geographic distribution of wells studied.

Cobb, 1975; Fertl and Wichmann, 1977; Harrison and others, 1983; Luheshi, 1983; Keho, 1987; Willett and Chapman, 1987; Cao and others, 1988; Deming, 1989; Deming and others, 1990; Prensky, 1992; Förster and Merriam, 1995; Blackwell and others, 1999; Förster, 2001; Andaverde and others, 2005; Zschocke, 2005; Goutorbe and others, 2007; Edwards, 2013; Morgan and Scott, 2014). This is a major reason BHTs should be considered low precision, low reliability data that need to be carefully evaluated (Willett and Chapman, 1987). Additionally, noise is a typical component of BHT data-sets for a wide range of reasons (Kehle and others, 1970; Luheshi, 1983; Speece and others, 1985; Cao and others, 1988; Deming and Chapman, 1988; Deming, 1989;

Deming and others, 1990; Förster and Merriam, 1995; Henrikson, 2000; Beardsmore and Cull, 2001; Henrikson and Chapman, 2002). In a deep well, the upper part of the well bore will frequently be heated while the lower section is cooled as drilling mud is circulated throughout the well bore (Guyod, 1946; Bullard, 1947; Glenn and others, 1980; Speece and others, 1985; Deming and others, 1990; Edwards, 2013). While the disturbed temperatures throughout the well bore will eventually re-equilibrate, the time required is typically 10 to 20 times the duration of the drilling, which may mean many months for deep wells (Bullard, 1947; Steeples and Stavnes, 1982; Luheshi, 1983; Beardsmore and Cull, 2001). The magnitude of the perturbation is smallest

at the bottom of the well near where temperatures are recorded (depending on the position of the thermometer on the tool string and other factors), but considerable time is still required to regain equilibrium temperatures (Deming and others, 1990; Blackwell and others, 1999; Henrikson, 2000; Henrikson and Chapman, 2002; Morgan and Scott, 2014). Unfortunately, geophysical logging in oil and gas wells is almost always initiated shortly (usually within 24 hours) after drilling and mud circulation has ceased, so the thermal disturbance is still great (Willett and Chapman, 1987; Prenskey, 1992; Beardsmore and Cull, 2001; Förster, 2001; Morgan and Scott, 2011; Edwards, 2013). Since oil and gas wells will typically be plugged and abandoned or in some other phase of development or production long before the well bore has time to recover to pre-drilling temperatures, numerous methods have been developed to correct for the drilling induced temperature disturbance.

## BHT DATA

### BHT Correction Methods

Hermanrud and others (1990) tested 22 methods developed between 1946 and 1988 against drill-stem test (DST) control data. Drill-stem tests typically draw fluids from some distance beyond the thermally disturbed volume of rock surrounding the well bore and are therefore commonly considered as a close approximation to the virgin rock temperature (VRT) (Harrison and others, 1983; Ben Dhia, 1988; Hermanrud and others, 1990; Förster and Merriam, 1995; Beardsmore and Cull, 2001; Shalev and others, 2008). However, DST reports sometimes record estimated temperatures, and other factors such as slow fluid flow and expanding gasses may decrease fluid temperatures and underestimate the VRT (Beardsmore and Cull, 2001). Ben Dhia (1988) notes other potential sources for error including the possibility that friction and compression could result in the overestimation of the VRT. Still, despite the potential inaccuracies, DSTs generally constitute the best available temperature data at depth. Unfortunately, DST data quantity is usually dwarfed by BHT data quantity and availability.

Goutorbe and others (2007), Crowell and Gosnold (2011), Crowell and others (2012), and Edwards (2013) compared various correction techniques. These comparison studies showed that most methods reliably estimate formation temperatures within about  $\pm 10^{\circ}\text{C}$  ( $\pm 18^{\circ}\text{F}$ ). Some methods are much more accurate but complex, requiring data that are rarely available. Many common methods use depth-dependent equations. These equations are typically derived from specific locations where sufficient quantities of DST or other reliable temperature data are used to develop an empirical correction, scaled by depth, which can be applied to an uncorrected BHT. Examples of these methods include Kehle and others (1970), Gregory and others, (1980), Harrison and others (1983), Willett and Chapman (1987), Ben Dhia (1988), Blackwell and Richards (2004), Förster and Merriam (1995), Morgan and Scott (2011, 2014), and

Crowell and others (2012). Because these methods were all derived for specific basins, they are not necessarily applicable to other sedimentary basins (Crowell and Gosnold, 2011; Crowell and others, 2012; Edwards, 2013; Morgan and Scott, 2014; Welhan and Gwynn, 2014).

Although a number of minor variations exist (mainly in certain assumptions that typically need to be made), Horner-type BHT corrections are commonly used in the petroleum industry and in geothermal investigations (Luheshi, 1983; Chapman and others, 1984; Hermanrud and others, 1990; Prenskey, 1992; Kutasov and Eppelbaum, 2005). The basis of these corrections is rooted in the work of Bullard (1947) and Lachenbruch and Brewer (1959), but the “Horner” name comes from the mathematically similar technique developed by Horner (1951) for examining pressure build-up in wells. Unlike the empirical methods that require only a single BHT measurement, Horner-type corrections are time-sequential, requiring BHT data from two or (preferably) more logging runs at the same depth. The premise of the technique is based on the formula from Chapman and others (1984): where:

$$T_B(t) = T_{B,\infty} + A \log \left( \frac{t_c + t_e}{t_e} \right) \quad (1)$$

$T_B(t)$  = the time-dependent BHT (in  $^{\circ}\text{C}$ ).

$T_{B,\infty}$  = temperature at infinite time (in  $^{\circ}\text{C}$ ).

$A$  = constant derived by linear regression for a given BHT set.

$t_c$  = the circulation time (in hr).

$t_e$  = the elapsed time since circulation stopped (in hr).

By plotting  $\log(t_c + t_e / t_e)$  against  $T_B(t)$  for two or more logging runs, the rate of temperature rebound can be extrapolated to infinite time, thereby providing an estimate of the undisturbed VRT.

Values for  $t_c$  are almost never recorded. So, in practice, most investigators use an estimated duration and apply it to all corrections (Deming, 1989). Undocumented values for  $t_e$  are another problem that frequently precludes using this method. Wells containing multiple time-temperature pairs needed for Horner-type corrections are uncommon in many locations. For example, Chapman and others (1984), Keho (1987), and Willett and Chapman (1987) found that only about 5% of the Uinta Basin wells were suitable for Horner-type corrections. Ben Dhia (1988), Shalev and others (2008), and Morgan and Scott (2014), describe similar situations for their investigations. Although not quantified, the proportion of wells suitable for Horner-type corrections in the Uinta Basin is still small despite a large increase in the number of wells drilled since the 1980s. This is due to logging tool developments that often allow all desired logs to be run concurrently.



Dowdle and Cobb (1975), Luheshi (1983), Hermanrud and others (1990), and Welhan and Gwynn (2014) suggest that Horner-type corrections tend to underestimate the VRT to some degree. However, we feel that for most geothermal studies, it is preferable to report more conservative (lower) VRT estimates.

Henrikson (2000) and Henrikson and Chapman (2002) used Horner-type corrections where possible, and then compiled those data to develop empirical correction equations that can be applied to wells where only a single time since circulation-temperature datum exists (i.e., BHTs from single logging runs at a given depth). Edwards (2013) compared the results of Horner-type corrections (assumed to represent the VRT) with the single-BHT equations of Henrikson (2000) and Henrikson and Chapman (2002). He found that the single-BHT corrections usually overcorrected by about 1°C (1.8°F) with a standard deviation of 11°C (19.8°F).

Horner and Horner-derived single point correction methods of Henrikson (2000) and Henrikson and Chapman (2002) have been used with reasonable success throughout Utah and surrounding states by Allis and others (2011, 2012), Edwards (2013), Gwynn and others (2013, 2014) and Welhan and others (2014). Within the inherent limitations of all BHT correction methods (see Deming, 1989 and Deming and others, 1990), we feel the Henrikson (2000) and Henrikson and Chapman (2002) methods provide reasonable estimated BHTs for the Uinta Basin.

### BHT Data Compilation

Of several thousand wells currently producing fluids, a sample of 776 were selected for this study (figure 1). Other thermal studies tend to combine thermal data from the Uinta Basin with data from the entire Colorado Plateau for a large-scale thermal regime such as in Henrikson (2000). In this study, wells were chosen to represent as much of the entire area of the Uinta Basin as possible in order to understand the thermal properties and regime on a basin-wide scale rather than a regional, lithospheric scale. However, the number of wells and spatial density of the data studied does not provide enough information for the research of shallow depth, intra-basin scale thermal characteristics.

Two sets of BHT data for the Uinta Basin were combined in this study. The first has data processed from 136 wells where sufficient, credible data were available to correct for the drilling-induced temperature perturbations using both Horner-type and single-point BHT correction methods of Henrikson (2000) and Henrikson and Chapman (2002) compiled for the National Geothermal Data System (NGDS) by the Utah Geological Survey. Many of these data were used by Chapman and others (1984), Keho (1987), and Willett and Chapman (1987) in previous heat-flow studies. These wells are primarily distributed among the Altamont-Bluebell-Cedar Rim oil fields in Duchesne County and Greater Natural Buttes field in Uintah County (Chapman and others, 1984;

Keho, 1987). Many of these wells had multiple data points at a given depth, allowing Horner-type corrections to be made, and are presumed to represent the highest-quality corrected BHTs in the study area. The correction factor assumes that the Horner-type correction provides a reliable estimate of the VRT in a given well (Fertl and Wichmann, 1977; Edwards, 2013).

Bottom-hole temperatures for the remaining 640 wells were extracted from geophysical logs via the online Utah Division of Oil, Gas, and Mining (DOGGM) database. A depth-dependent correction factor specific to the Uinta Basin was derived and applied to the uncorrected BHTs of this dataset. This correction factor was determined using Horner-corrected BHTs from the 136 previously corrected wells. The difference between each uncorrected BHT and the Horner-corrected temperature was calculated and the average of these values was found to be 2.0°C/km (0.11°F/100 ft). This correction, a linear function of depth, was applied to the remaining 640 wells.

These corrections, though less rigorous than the other methods, generally result in corrected gradients very similar to those of the first dataset. Therefore, we feel confident that the corrected BHTs in this dataset are reasonable, especially when viewed with the inherent limitations and uncertainties of BHT data. Together, the two datasets generate a BHT database of 776 wells within the Utah portion of the Uinta Basin (figure 2) that is left-skewed, normally distributed around a mean BHT of about 96°C (205°F).

### Heat Flow

In this study, corrected BHTs are combined with additional thermal data and used as inputs of the Simple Gradient and Thermal Resistance Methods (figure 3) for calculating one-dimensional heat-flow values following Chapman and others (1984), Keho (1987), and Henrikson (2000). The thickness of lithofacies encountered in each well in this study were taken from existing UGS data. Thermal conductivity values directly measured by the divided-bar method are taken from Keho (1987) and Henrikson (2000) when available. Otherwise, lithofacies were assigned a typical thermal conductivity value sourced from common industry data compiled by Beardsmore and Cull (2001). Mean annual surface ground temperature (SGT) values for each well were extrapolated from Edwards (2013). First, a thermal gradient is calculated using the Simple Gradient Method given by:

$$T_B = T_0 + \left( \frac{\partial T}{\partial Z} \right) B \quad (2)$$

where:

$T_B$  = the temperature at depth  $B$  (in °C).

$T_0$  = the mean annual surface ground temperature (in °C).

$(\partial T / \partial Z)$  = the thermal gradient (in °C/m).

$B$  = the depth the BHT was recorded (in m).



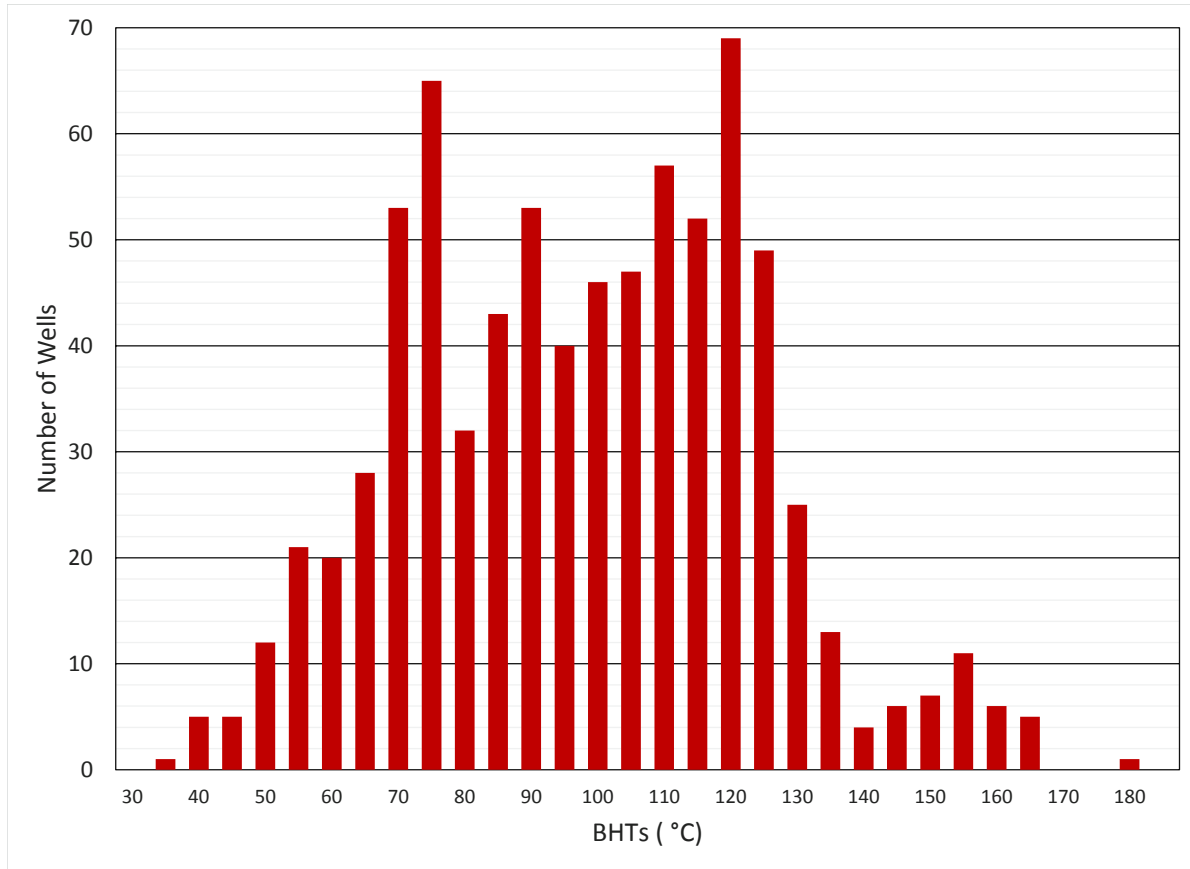


**Figure 2.** Histogram showing the distribution of bottom-hole temperatures (BHT).

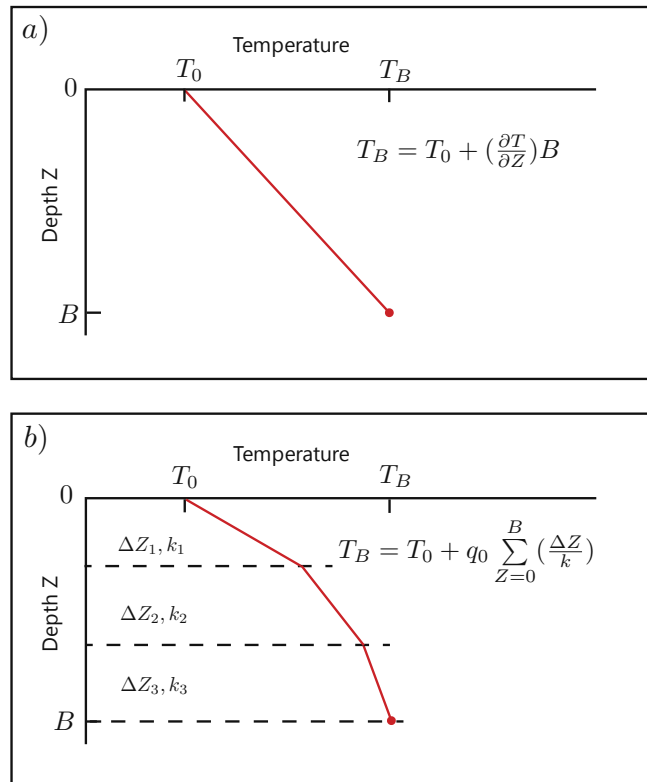


**Figure 3.** Simple Gradient (a) and Thermal Resistance Method (b) plots (modified from Chapman and others, 1984).

An initial estimate of heat flow based on the Simple Gradient Method and Fourier's Law is then computed using the calculated gradient and a thickness weighted (arithmetic) mean of thermal conductivities,  $k$ , for all stratigraphic layers within the gradient interval. Fourier's law of heat conduction in 1D is:

$$q_0 = k \frac{\partial T}{\partial Z} \quad (3)$$

where:

$q_0$  = surface heat flow (in W/m<sup>2</sup>).

$k$  = thermal conductivity (in W/mK).

$(\partial T/\partial Z)$  = the thermal gradient (in °C/m).

With this estimate, a starting value of surface heat-flow is determined and then used in the Thermal Resistance Method. The thermal resistance is the relation between a lithological unit of thickness  $\Delta z$  and the associated thermal conductivity  $k$ . This method allows for lateral differences in subsurface temperature, thermal conductivity, and heat flow which does not restrict oil and gas fields to a homogenized, single gradient or conductivity value. The governing equation for the Thermal Resistance Method is:

$$T_B = T_0 + q_0 \sum_{z=0}^B \left( \frac{\Delta z}{k} \right) \quad (4)$$

where:

- $T_B$  = the temperature at depth where  $z = B$  (in °C).  
 $T_o$  = the mean annual SGT at each well location (in °C).  
 $q_o$  = surface heat flow (in W/m<sup>2</sup>).  
 $\Delta z$  = the vertical interval (in m).  
 $k$  = thermal conductivity (in W/mK).

Thermal resistance is summed for all layers between the surface and depth  $B$  (Keho, 1987) to compute the temperature value at  $B$  (also known as bootstrapping). In this study, temperature is calculated with the Thermal Resistance Method in an iterative, forward-modeling approach by adjusting the heat-flow parameter which is guided by the residual of the observed and calculated BHTs until the data are within a tolerance of 1%. The Thermal Resistance Method gives a better approximation for the final surface heat-flow value compared to the Simple Gradient Method because it incorporates all subsurface layers in the computation.

### Heat Flow Results

The Thermal Resistance Method was applied to the 776 wells in this study (figure 4). The mean surface heat flow for all wells studied is 67 mW/m<sup>2</sup> with a standard deviation of 12 mW/m<sup>2</sup>. The mean thermal gradient for the data is 31°C/km (1.7°F/100 ft) with a standard deviation of 6°C/km (0.33°F/100 ft). However, these data reveal the presence of several anomalous wells with heat-flow values exceeding 100 mW/m<sup>2</sup>. While some spatial variation is expected, a single well with a heat-flow value on

the order of 50 mW/m<sup>2</sup> greater than several neighboring wells is unlikely. Many of these wells were eliminated from the final calculations due to potentially erroneous BHT data based on comparing the heat flow of an anomalous well to that of several neighboring wells. A heat flow value of  $65 \pm 10$  mW/m<sup>2</sup> and a mean geothermal gradient of  $27 \pm 5^\circ\text{C/km}$  ( $1.48 \pm 0.27^\circ\text{F/100 ft}$ ) were calculated after filtering the anomalous wells (Figures 5 and 6).

The mean surface heat flow falls within a reasonable range when compared with previous studies, although the overall accuracy could be improved with additional high-quality BHT data. A heat-flow study detailed by Chapman and others (1984) and Keho (1987) of 97 wells located primarily in the northwest portion of the Uinta Basin resulted in a mean heat flow of 57 mW/m<sup>2</sup>  $\pm 11$  mW/m<sup>2</sup> from a range of 40 to 65 mW/m<sup>2</sup>. A study of the entire Colorado Plateau by Henrikson (2000) reports a mean heat-flow value of 62 mW/m<sup>2</sup>  $\pm 2$  mW/m<sup>2</sup> which includes around 100 heat-flow values for the Uinta Basin. Keho (1987) and Henrikson (2000) used fewer, but more accurate, BHTs in their work, which may partly explain the differences. Another factor may be our use of more wells spread over a greater expanse of the Uinta Basin, a major goal of this study.

## THERMAL MODELS

### Background Data and Methods

Building upon the observed and computed thermal data described above, we created a conductive thermal model of the Uinta Basin using COMSOL Multiphysics 4.4, a finite element method modeling program. This initial thermal model is intended to bracket the regional back-

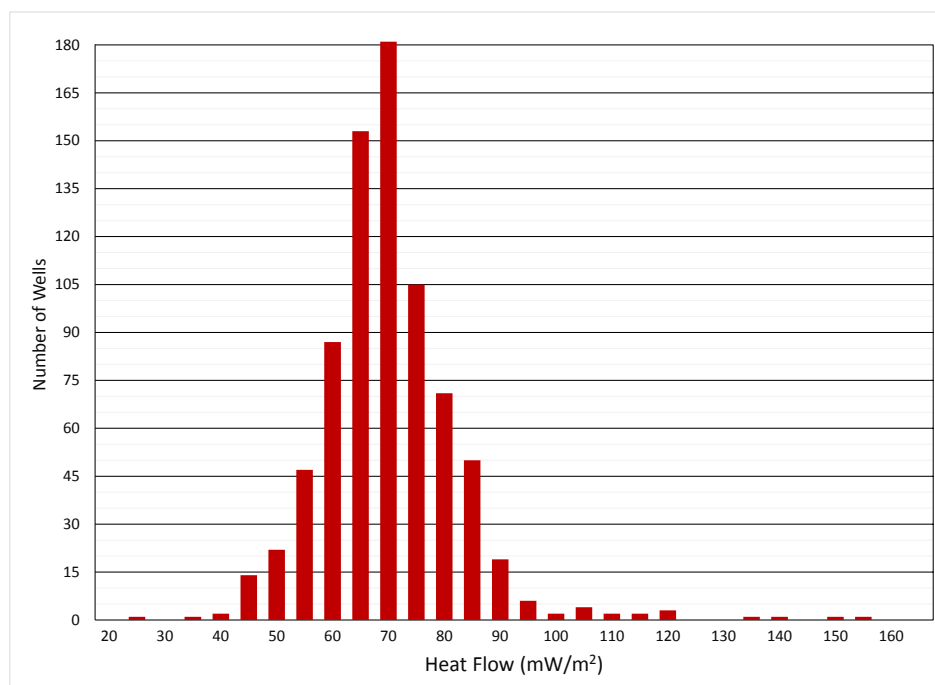


**Figure 4.** Histogram showing the distribution of calculated heat-flow values.

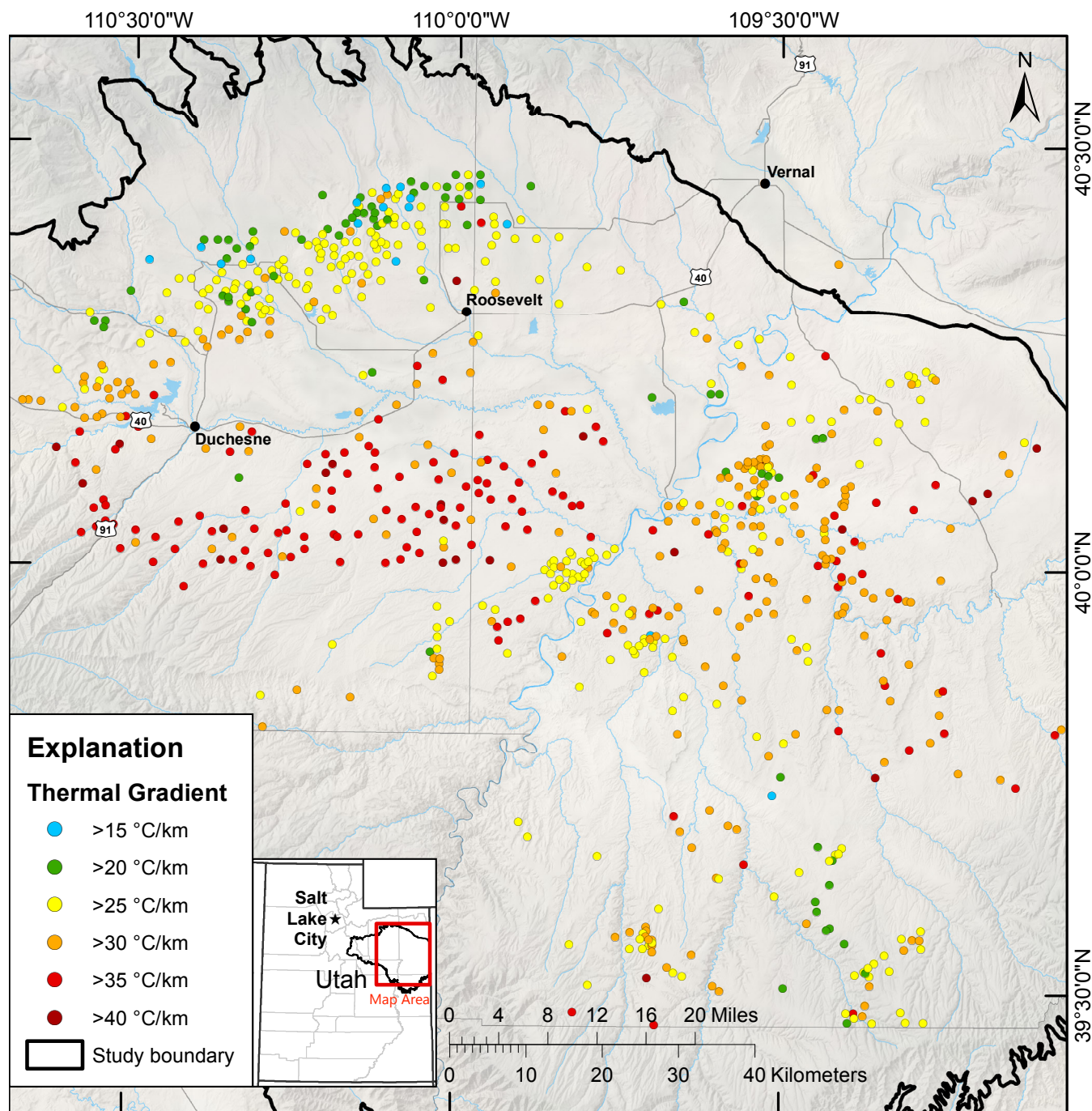


**Figure 5.** Thermal gradients of oil and gas wells. These wells, categorized by corrected BHTs, show the general trend of thermal gradients in the Uinta Basin. Gradients are slightly higher than the average of 27°C/km (1.48°F/100 ft) along the center of the basin with cooler than average gradients to the north and south. Gradients may be cooler along the northern margins due to groundwater recharge from the south flank of the Uinta Mountains.

ground heat flow so that more detailed models exploring spatial heterogeneities can be developed. The methods used by Hardwick and others (2014) to generate a similar model of the Black Rock Desert of Utah were used in this study. Model framework (figure 7) consists of surface topography from a 5-meter digital elevation model, a basement interface as determined by well data, and isopach maps from previous UGS Uinta Basin research. In this study, a simple layer-cake model is implemented consisting of only two material layers (basement rock and

basin-fill material). In areas where basin-fill thickness is zero, we set the bedrock contact at 10 meters depth so that the layers are continuous without any overlap. Model layers are then smoothed within COMSOL in order to simplify the meshing and speed up computing time. We use the mean annual SGT from Edwards (2013) as the upper boundary condition and a spatially uniform basal heat flux as the lower boundary condition. Both boundary conditions are invariant with respect to time.



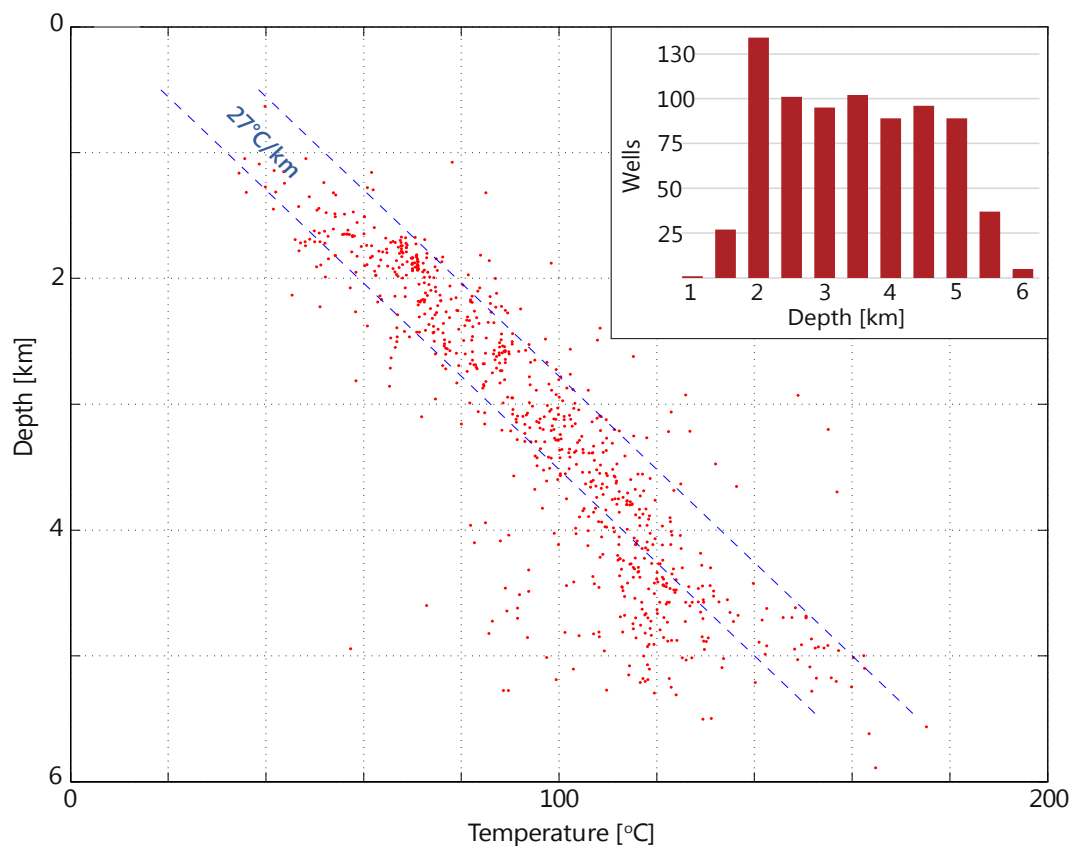


**Figure 6.** Temperatures at depth. The average thermal gradient of 27°C/km (1.48°F/100 ft) is bracketed over a range of surface temperatures. Well depth distribution in upper-right corner.

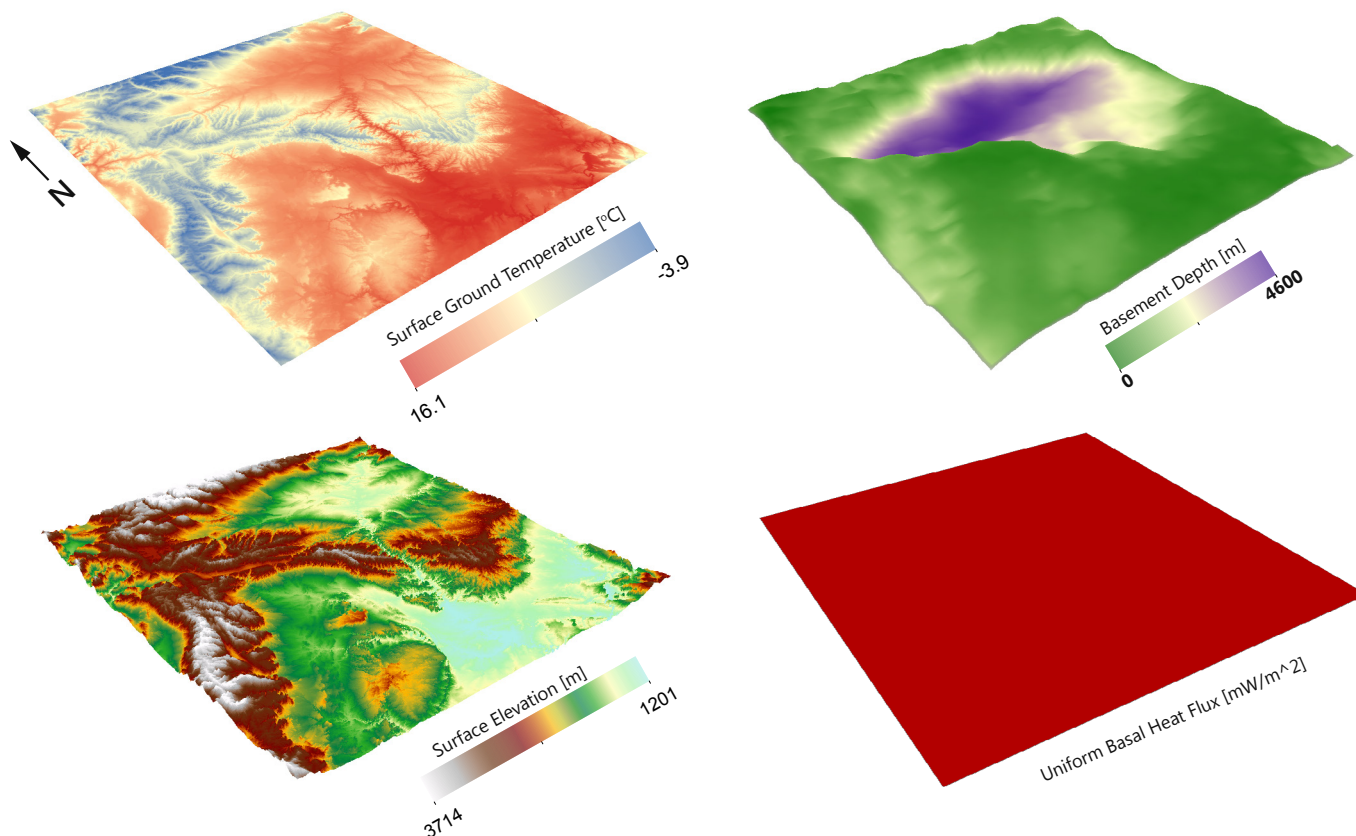


**Figure 7.** Thermal model framework including upper and lower boundary conditions.

The range of thermal conductivities chosen for the model are determined by the measured properties of core and cutting samples recovered from Uinta Basin wells (Keho, 1987; Henrikson, 2000) and typical values for the lithology recorded in the well logs. Thermal conductivities for the basin fill layer ( $k_1$ ) range from 2.0 to 3.0 W/mK (9 total) and for the basement rock layer ( $k_2$ ) range from 3.5 to 4.5 W/mK (9 total). Increments of 0.125 W/mK were modeled for each layer. The lower boundary condition, basal heat flow ( $q_b$ ), is uniform and a range of values from 60 to 80 mW/m<sup>2</sup> are used (5 total). The upper and lower limits of the range for all parameters are intentionally extended slightly beyond known values as a check of the model behavior and to help define global and local minimums. A parametric sweep scheme using COMSOL results in 81 models per  $q_b$  value (405 models in total).

### Model Results and Discussion

Temperature and heat-flow residuals (figure 8) indicate where the thermal models correlate with the observed data. The residuals are computed from 776 observed subsurface temperature points and the respective surface heat-flow values compared to the modeled temperatures at the same locations reported as the mean, standard deviation, and maximum difference. Temperature residuals show that the models are more sensitive to changes in the basin-fill thermal conductivity than to changes in basement rock. This is expected because the Uinta Basin is a deep basin (exceeding 4.5 km [14,760 ft]) and the primary effects on temperature are the insulating properties of the basin-fill material. The 70 mW/m<sup>2</sup> basal heat-flow value results in the best-fit models according to temperature residuals and shows a global minimum for the  $k_1$  parameter. This overall best-fit model uses  $k_1=2.375$  and  $k_2=4.0$ , with residuals of 9.8, 9.0, and 61.9°C (50, 48, and 143°F) for mean, standard deviation, and maximum.

Heat-flow residuals vary only slightly for changes in  $k_1$  and  $k_2$  values. As with the temperature residuals, the basal flux of 70 mW/m<sup>2</sup> contains the best-fit model as well as the lowest model residuals for all combinations of  $k_1$  and  $k_2$  compared to other basal-flux values. The best-fit basal flux model for heat-flow residuals has the same  $k_1$  and  $k_2$  values as the best temperature residual model. The heat-flow residuals are 8.0, 7.0, and 46.0 mW/m<sup>2</sup> for the mean, standard deviation, and maximum difference.

Temperature slices at depth shown in figure 9 of the Uinta Basin thermal model are produced at approximate depths of 2, 3, 4, and 5 km (6560, 9840, 13,120, and 16,400 ft) below the average surface elevation of the basin. For an area of 16,000 km<sup>2</sup> (6180 mi<sup>2</sup>) we find that temperatures are generally greater than 75°C (167°F) at a depth of 2 km (6560 ft) and in some areas exceed 100°C (212°F). In this assessment, the calculated minimum temperature required for direct-use applications (greenhouses, etc.) is 50°C (122°F) which is met at 2 km (6560 ft) depth in the entire basin model. Modeled

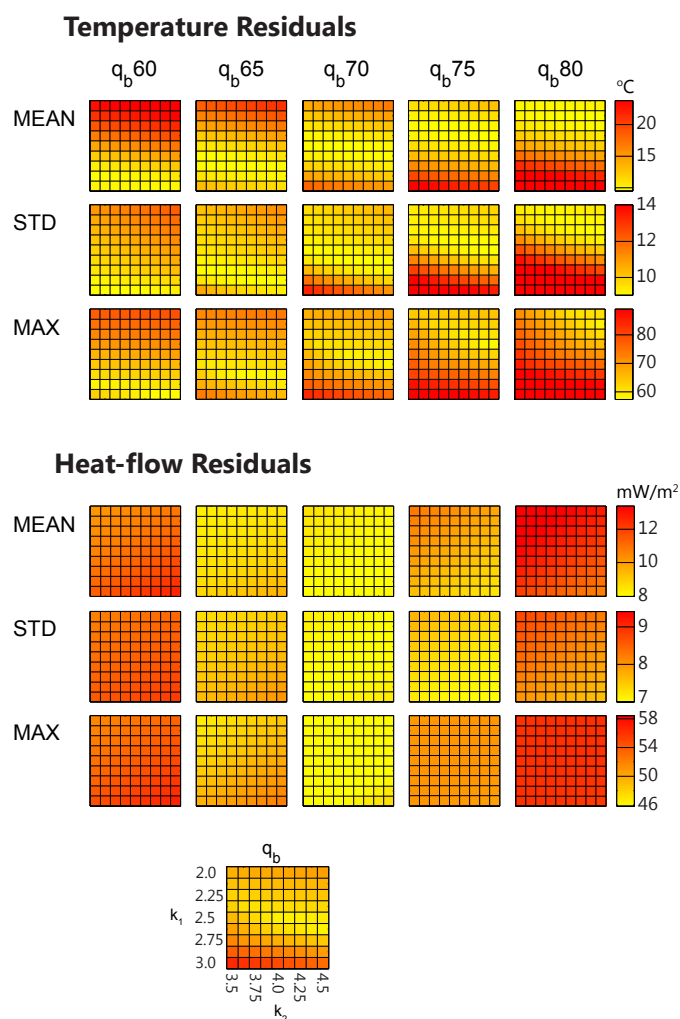


**Figure 8.** Residuals of model results to observed data for each model parameter set represented as mean, standard deviation, and maximum. Top panel shows temperature residuals and bottom panel shows surface heat-flow residuals.

temperatures reach 150°C (302°F) at a depth of 5 km (16,400 ft) below the basin, which exceeds the minimum temperature of 140°C (284°F) required for binary geothermal power production.

The modeled surface heat flow in the Uinta Basin ranges from 50 to over 80 mW/m<sup>2</sup> (figure 10). Values are generally highest in the mountains and lowest in the valleys. Due to the refraction of heat flow along the basin/basement interface, we expect bedrock values to exceed the uniform basal flux of 70 mW/m<sup>2</sup>. This is observed in the model along the margins of the Uinta Basin where basin-fill thickness is thin and bedrock is at or near the surface. Average heat flow for the Uinta Basin using the thermal resistance method is 67 mW/m<sup>2</sup>, which agrees reasonably with the best-fit thermal model and suggests that the thermal regime of the basin may be primarily conductive.

When comparing the 3D model to the 1D calculations there are some key differences to point out. Since the

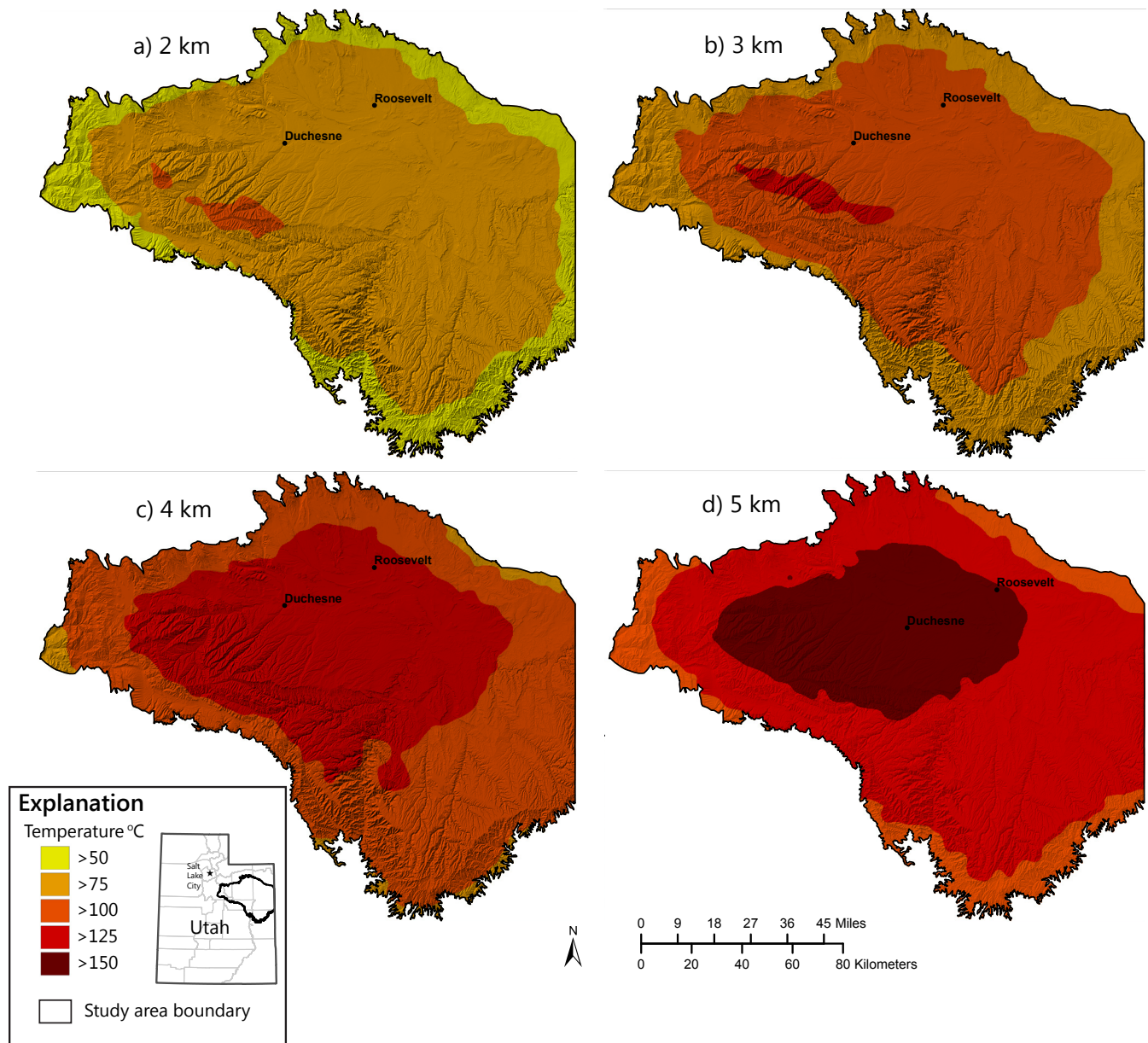


**Figure 9.** Maps of the temperature field at planes of constant elevation below the average elevation of the Uinta Basin.

primary intention of the initial 3D model is to constrain the background regional heat flow, disparities are expected when examined against the 1D values. These differences can typically be the result of heat transport in modes other than that of conduction (i.e., advection, convection). We find that differences are most prominent at the northern end of the Uinta Basin where the thermal model over predicts the 1D values by up to 30 mW/m<sup>2</sup> or more. One proposed explanation for this difference is that regional groundwater flow is flushing the heat (cooling the host rock) via recharge pathways originating in the Uinta Mountains and moving southward into the basin. This hypothesis of groundwater flow is also suggested by a number of saline water studies of the Uinta Basin (Howells and others, 1987; Freethey, 1992; Glover, 1996; Zhang and others, 2009; Anderson and others, 2012) in order to explain the great depth to the

base of the saline water in the northern Uinta Basin. We find that this deep trend is coincident with low heat-flow values (figure 11) and most likely a cause and effect relationship. An east-west trend of under predicted heat flow is observed through the central part of the basin where model results are lower than 1D values by 15 mW/m<sup>2</sup> on average. This trend aligns with the Duchesne fault zone as well as a shallow trend of the moderately saline fluid base. The shallow base is thought to be related to the upward mobility of fluids enabled by the fault-and-fracture system (among other factors) according to Anderson and others (2012). Heat transport within these upward moving fluids could explain the elevated heat flow in the central part of the basin, coincident with the Duchesne fault zone. In order to facilitate a more in-depth study of the Uinta Basin, revised versions of the 3D thermal models should incorporate fluid flow to better address



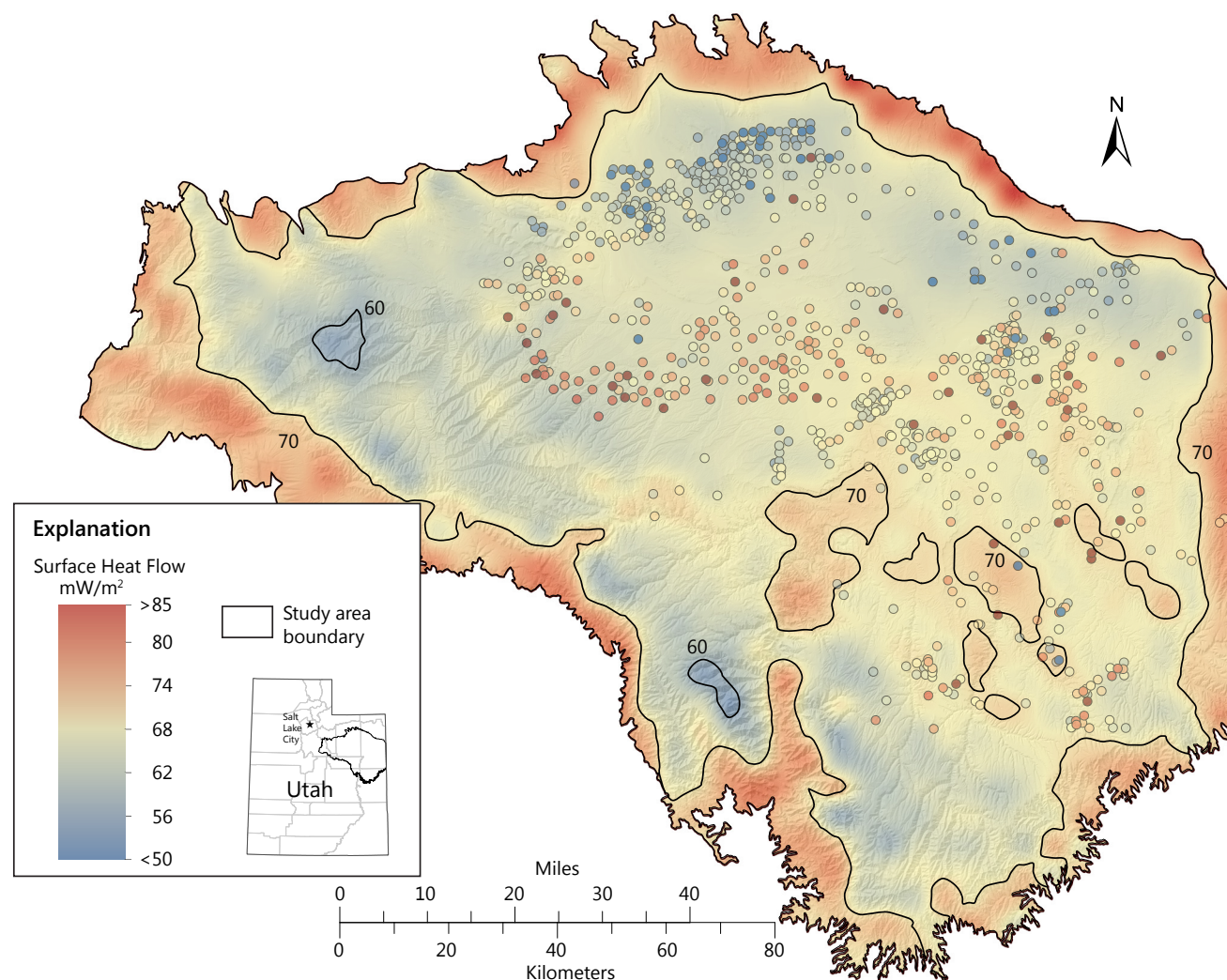


**Figure 10.** Surface heat flow from Uinta Basin thermal model and corrected well data (symbols colored according to heat-flow values). Black lines are contours of heat flow in 10 mW/m<sup>2</sup> intervals.

the effects of the groundwater flow hypotheses.

## GEOHERMAL RESOURCE POTENTIAL

This study shows that co-produced fluids from oil and gas wells within the Uinta Basin may represent a significant, yet unused, geothermal resource. The mean thermal gradient of 27°C/km (1.48°F/100 ft) for the Uinta Basin implies that any well deeper than 2 km (6500 ft) could have a fluid temperature of about 65°C (149°F) when using a mean annual SGT of 11°C. This temperature is well above the minimum threshold required for heated fluids to be used in direct-use applications such as aquaculture, greenhouses, and space heating (Boyd, 2008). Since the average depth of wells in this study is 3 km (9840 ft), higher temperatures can be expected from the majority of producing wells.

Fluid production volumes from Uinta Basin wells have been averaged using available data, which, in many cases, represents the entire production period for a given well. With documented flow and temperature values, we

can calculate the heat content and thermal output of each well. The heat-energy content can be calculated by:

$$Q = mc\Delta T \quad (5)$$

where:

- $m$  = the mass of the fluid (in kg).
- $c$  = 4200 J/kgK (the specific heat of water).
- $\Delta T$  = the change in temperature from produced depth to surface (in °C).

Applying this equation to our Uinta Basin dataset results in an average thermal output of 88 kW, but a maximum output of up to 10 MW (a well in the Ashley Valley field near Vernal) was calculated for wells with exceptionally high volumes of produced fluids (figure 12). Of the wells studied, 587 of the 776 fall in a range of 25 to 100 kW of thermal output. The most significant parameter affecting thermal output is the volume of produced fluid, which varies significantly in the Uinta Basin. Slighter higher fluid output volume would drastically increase

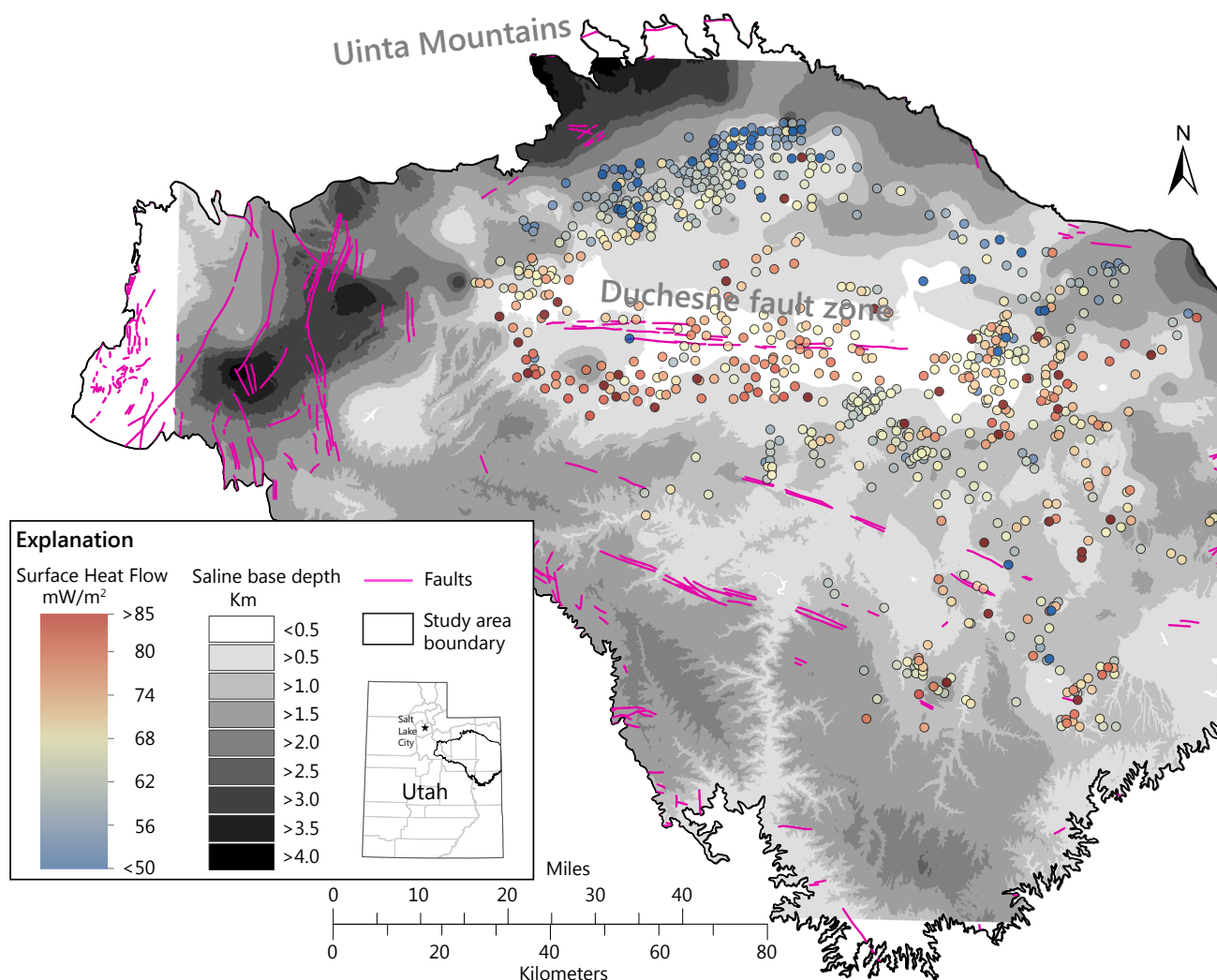


**Figure 11.** Map of depth in km to the base of the moderately saline water (data from Anderson and others, 2012) in the Uinta Basin. Well locations and calculated heat-flow values (symbols colored according to heat-flow values) are shown. Magenta lines are faults. A noticeable spatial correlation between the depths to the base of the moderately saline water and heat flow can be observed. Heat-flow values are lower in the northern area where the base to the saline water is deep and heat-flow values are higher in the central part of the basin where the base to the saline water is shallow.

thermal power output.

Binary geothermal power systems are commonly used to generate electricity from intermediate-temperature reservoirs. Resource fluid temperatures between 120°C and 150°C (248°F and 302°F) are suitable for binary-cycle power plants (Blackett and others, 2004). In a binary system, geothermal water passes through a heat exchanger to heat a secondary working fluid. This working fluid flashes to steam at a lower temperature and pressure than water and is used to drive the generator turbine. The cooled geothermal fluid is then injected back into the geothermal reservoir. Temperatures above 120°C (248°F) are found in 127 wells in our dataset. However, useable heat content is limited by the temperature difference between the surface and the production depth. In addition, the efficiency of existing geothermal power plants demonstrates that a resource temperature

at or above 140°C (284°F) is preferred (Blackett and others, 2004). Such temperatures are observed in 36 wells in this study, so geothermal power generation may be viable from wells with sufficient fluid production and adequate temperature (figure 13).

Alternatively, produced fluids could be used for direct-use geothermal applications such as greenhouse heating. The Newcastle area near Cedar City, Utah, currently sustains nine greenhouses covering an area of 3135 m<sup>2</sup> (33,750 ft<sup>2</sup>) growing crops in a hydroponic system (Boyd, 2008). However, the resource may be able to sustain greenhouses covering an area up to 100,000 m<sup>2</sup> (1.1 million ft<sup>2</sup>, 25 acres) according to findings from Blackett and others (2004). Greenhouse heating requirements are highly variable depending on several factors including, but not limited to, greenhouse size/volume, structural materials, heat delivery methods, crop requirements, and weather

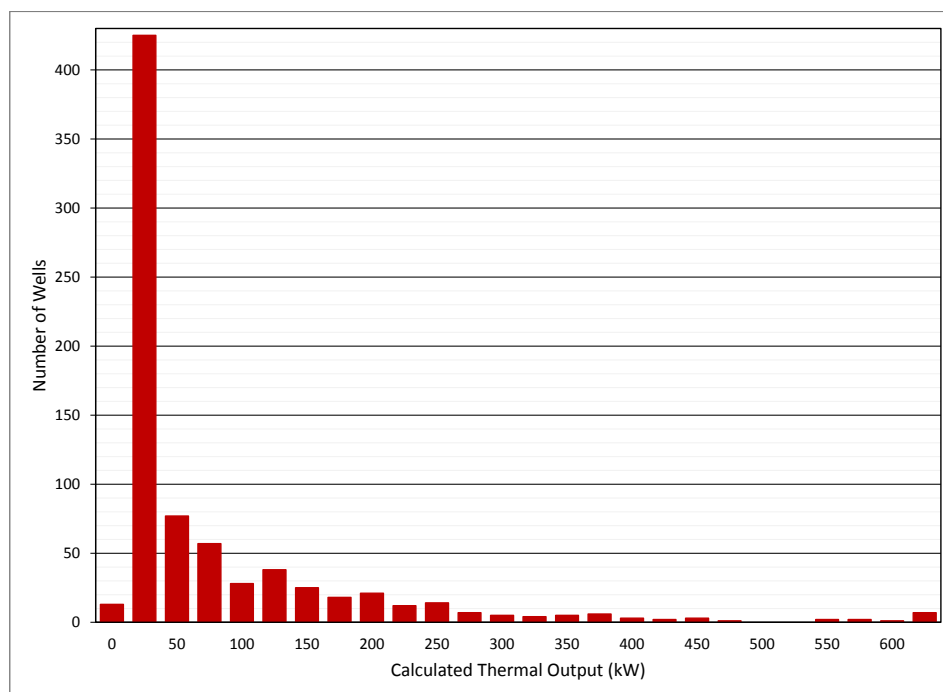


**Figure 12.** Histogram showing the distribution of calculated thermal output.

(Boyd, 2008). We can, in general, compute peak energy requirements by using the following equation:

$$Q_g = AU\Delta T \quad (6)$$

where:

- $Q_g$  = the total energy requirement (in J).
- $A$  = the area of the green house construction material (in  $m^2$ ).
- $U$  = the heat loss factor of the greenhouse material (unitless).
- $\Delta T$  = the change in temperature from mean annual SGT and the desired internal temperature (in  $^{\circ}C$ ).

A common type of greenhouse is the fiberglass-plastic style, where the walls are made of fiberglass and a domed roof is made of a double layer of plastic film enclosing an air space. Such a greenhouse covering an area of 468  $m^2$  (5037  $ft^2$ ) would require 51 kW (174,676 Btu/hr) of power to maintain an internal temperature of 21 $^{\circ}C$  (70 $^{\circ}F$ ) with a mean external temperature of 10 $^{\circ}C$  (50 $^{\circ}F$ ). Additional design parameters from Boyd (2008) and Lund (2011) reveal that a single well must produce 3 to 5  $m^3/hr$  (10–22 GPM) of >50 $^{\circ}C$  (122 $^{\circ}F$ ) fluids to sustain the greenhouse described above. It should be noted this is a general calculation and specific greenhouse requirements vary according to materials, location, and desired crop to be grown. Minimum temperatures are found in 740 wells in our dataset, and 29 of these also meet the flow requirements of our example greenhouse. These wells could support 86 greenhouses (figure 13). Regardless of volumetric production, the high number of existing wells producing fluids above 50 $^{\circ}C$  (122 $^{\circ}F$ ) make

direct-use geothermal applications (i.e., greenhouses) in the Uinta Basin an attractive option.

## CONCLUSIONS

This geothermal assessment of the Uinta Basin presents encouraging results related to geothermal potential in a number of ways. With a well-distributed sampling of thermal data in the Uinta Basin, we are able to identify key thermal characteristics that are important to geothermal prospecting and the possibility of future development. Average background heat flow of 67  $mW/m^2$  and an average geothermal gradient of 27 $^{\circ}C/km$  (1.48 $^{\circ}F/100$  ft) result in adequate temperatures (>50 $^{\circ}C$  [122 $^{\circ}F$ ]) at depths greater than 2 km (6562 ft) for direct-use applications such as greenhouses. This is important because of the large number of wells that are deeper than 2 km and the pre-existing well infrastructure (significant cost savings for development) in the basin. Preliminary thermal models of the Uinta Basin give some support to existing interpretations that the thermal regime is primarily conductive with the exception of groundwater flushing from the Uinta Mountains. A conductive regime implies that the thermal aspects, intra-basin systems and responses are more predictable and likely are uniformly spread across the basin, resulting in a larger geothermal prospect. Future models incorporating basin-scale fluid flow will provide better estimates of the resource potential within the basin. From this small subset of Uinta Basin well data, we find 740 wells meeting the temperature requirement of 50 $^{\circ}C$  (122 $^{\circ}F$ ) for direct-use applications and 36 wells meeting the temperature requirement of 140 $^{\circ}C$  (284 $^{\circ}F$ ) for binary geothermal power production.



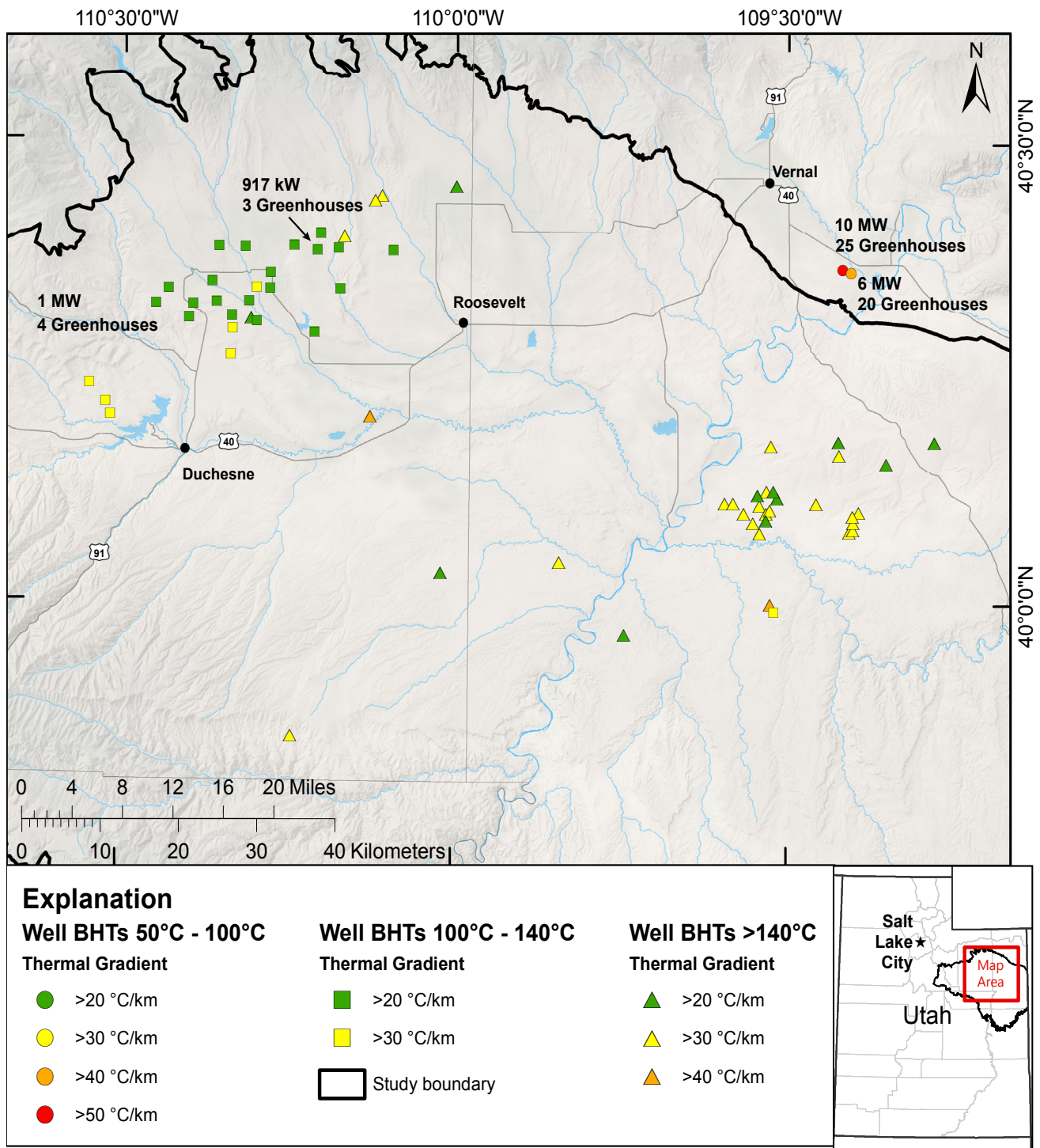


**Figure 13.** Map of wells co-producing water at a sufficient volume to support at least one 468 m<sup>2</sup> (5037 sq ft) greenhouse (square symbol, indicated when more than three can be supported) and wells meeting required temperature threshold (>140°C) for binary power generation (triangles). The potential is greatest for wells in the Ashley Valley field near Vernal, in the northwest quadrant of the map, due to high volumetric output of co-produced fluid.

The average thermal output per well is 88 kW and maximum output is as high as 10 MW. For each well, as produced oil volumes decrease and co-produced fluids increase and the door opens to even more geothermal resource that could be used locally.

## ACKNOWLEDGEMENTS

The authors would like to thank the members of the Utah Geological Survey for their contributions to this manuscript. Funding for this ongoing research is provided

by Research Partnership to Secure Energy for America (RPSEA), contract number 11123-08. Additional funding was provided by the Utah Geological Survey.

## REFERENCES

- Allis, R., Blackett, R., Gwynn, M., Hardwick, C., Moore, J.N., Morgan, C., Schelling, D., and Sprinkel, D., 2012, Stratigraphic reservoirs in the Great Basin—the bridge to enhanced geothermal systems in the U.S.: Transactions, Geothermal Resources Council, v. 36, p. 351–357.
- Allis, R., Moore, J., Blackett, B., Gwynn, M., Kirby, S., and Sprinkel, D., 2011, The potential for basin-centered geothermal resources in the Great Basin: Transactions, Geothermal Resources Council, v. 35, p. 683–688.
- Andaverde, J., Verma, S.P., and Santoyo, E., 2005, Uncertainty estimates of static formation temperatures in boreholes and evaluation of regression models: Geophysics Journal International, v. 160, p. 1112–1122.
- Anderson, P.B., Vanden Berg, M.D., Carney, S., Morgan, C., and Heuscher, S., 2012, Moderately saline groundwater in the Uinta Basin, Utah: Utah Geological Survey Special Study 144, 30 p.
- Beardsmore, G.R., and Cull, J.P., 2001, Crustal heat flow—a guide to measurement and modeling: Cambridge, Cambridge University Press, 334 p.
- Ben Dhia, H., 1988, Tunisian geothermal data from oil wells: Geophysics, v. 53, no. 11, p. 1479–1487.
- Blackett, R.E., Sowards, G.M., and Trimmer, E., 2004, Utah's high temperature geothermal resource potential—analysis of selected sites: Utah Geological Survey Open File Report, 124 p.
- Blackwell, D.D., Beardsmore, G.R., Nishimori, R.K., and McMullen, R.J., Jr., 1999, High resolution temperature logs in a petroleum setting—examples and applications, *in* Förster, A., and Merriam, D.F., editors, Geothermics in basin analysis: New York, Plenum Press, p. 1–34.
- Blackwell, D.D., and Richards, M., 2004, Calibration of the AAPG geothermal survey of North America BHT data base: American Association of Petroleum Geologists Annual Meeting, Dallas, Texas, April 18–24, 2004, Poster Session, Extended Abstract 87616.
- Boyd, T., 2008, Geothermal greenhouse information package: Oregon Institute of Technology, 287 p.
- Bullard, E.C., 1947, The time necessary for a borehole to attain temperature equilibrium: Monthly Notices, Royal Astronomical Society, Geophysical Supplement, v. 5, no. 5, p. 127–130.
- Cao, S., Lerche, I., and Hermanrud, C., 1988, Formation temperature estimation by inversion of borehole measurements: Geophysics, v. 53, p. 979–988.
- Chapman, D.S., Keho, T.H., Bauer, M.S., and Picard, D.M., 1984, Heat flow in the Uinta Basin determined from bottom hole temperature (BHT) data: Geophysics, v. 49, no. 4, p. 453–466.
- Clem, K., 1985, Oil and gas production summary of the Uinta Basin, *in* Picard, M.D., editor, Geology and energy resources, Uinta Basin of Utah: Salt Lake City, Utah Geological Association Publication 12, p. 159–167.
- Crowell, A.M., and Gosnold, W., 2011, Correcting bottom-hole temperatures—a look at the Permian Basin (Texas), Anadarko and Arkoma Basins (Oklahoma), and Williston Basin (North Dakota): Transactions, Geothermal Resources Council, v. 35, p. 735–738.
- Crowell, A.M., Ochsner, A.T., and Gosnold, W., 2012, Correcting bottom-hole temperatures in the Denver Basin—Colorado and Nebraska: Transactions, Geothermal Resources Council, v. 36, p. 201–206.
- Deming, D., 1989, Application of bottom-hole temperature corrections in geothermal studies: Geothermics, v. 18, no. 5/6, p. 775–786.
- Deming, D., and Chapman, D.S., 1988, Inversion of bottom-hole temperature data—the Pineview field, Utah-Wyoming thrust belt: Geophysics, v. 53, no. 5, p. 707–720.
- Deming, D. and Chapman, D.S., 1989, Thermal histories and hydrocarbon generation—examples from Utah-Wyoming thrust belt: American Association of Petroleum Geologists Bulletin, v. 73, no. 12, p. 1455–1471.
- Deming, D., Nunn, J.A., Jones, S., and Chapman, D.S., 1990, Some problems in thermal history studies, *in* Nuccio, V.F., and Barker, C.E., editors, Applications of thermal maturity studies to energy exploration: Rocky Mountain Section, Society for Sedimentary Geology, p. 61–80.
- Dowdle, W.L., and Cobb, W.M., 1975, Static formation temperature from well logs—an empirical method: Journal of Petroleum Technology, v. 27, no. 11, p. 129–135.
- Edwards, M.C., 2013, Geothermal resource assessment of the Basin and Range Province in western Utah:

- Salt Lake City, University of Utah, M.S. thesis, 133 p.
- Fertl, W.H., and Wichmann, P.A., 1977, How to determine static BHT from well log data: *World Oil*, v. 184, p. 105–106.
- Förster, A., 2001, Analysis of borehole temperature data in the northeast German Basin—continuous logs versus bottom-hole temperatures: *Petroleum Geoscience*, v. 7, p. 241–254.
- Förster, A., and Merriam, D.F., 1995, A bottom-hole temperature analysis in the American Midcontinent (Kansas)—implications to the applicability of BHTs in geothermal studies, in *World Geothermal Congress 1995*, Firenze, Italy, May 18–31, 1995, *Proceedings: International Geothermal Association*, v. 2, p. 777–782.
- Freethy, G.W., 1992, Maps summarizing geohydrologic information in an area of salt-water disposal, eastern Altamont-Bluebell petroleum Field, Uinta Basin, Utah: U.S. Geological Survey Water Resource Investigation Report 92-4043, 2 plates.
- Glenn, W.E., Chapman, D.S., Foley, D., Capuano, R.M., Cole D., Sibbett, B., and Ward, S.H., 1980, Geothermal exploration program Hill Air Force Base, Davis and Weber Counties, Utah: U.S. Department of Energy Report, Contract DE-AC07-78ET28392, 77 p.
- Glover, K.R., 1996, Ground-water flow in the Duchesne River–Uinta aquifer in the Uinta Basin, Utah and Colorado: U.S. Geological Survey Water Resource Investigation Report 92-4161, p. 24.
- Goutorbe, B., Lucazeau, F., and Bonneville, A., 2007, Comparison of several BHT correction methods—a case study on an Australian data set: *Geophysics Journal International*, v. 170, no. 2, p. 913–922.
- Gregory, A.R., Dodge, M.M., Posey, J.S., and Morton, R.A., 1980, Volume and accessibility of entrained (solution) methane in deep geopressed reservoirs—Tertiary formations of the Texas Gulf Coast: U.S. Department of Energy Final Report DOE/ET/11397-1, 361 p.
- Guyod, H., 1946, Temperature well logging [a seven-part series]: *Oil Weekly*, v. 123, no. 8–11, (October 21, 28; November 4, 11), v. 124, no. 1–3 (December 2, 9, 16).
- Gwynn M., Allis, R., Blackett, R., and Hardwick, C., 2013, New geothermal resource delineated beneath Black Rock Desert, Utah, in *Thirty-Eighth Workshop on Geothermal Reservoir Engineering*, Stanford, California, February 11–13, 2013, *Proceedings: Stanford University, SGP-TR-198*, 9 p.
- Gwynn, M., Allis, R., Sprinkel, D., Blackett, R., and Hardwick, C., 2014, Geothermal potential in the basins of northeastern Nevada: *Transactions, Geothermal Resources Council*, v. 38, p. 1029–1039.
- Hardwick, C.L., Kirby, S., and Gwynn, M., 2014, Geothermal prospecting in Utah—a new thermal model of the Black Rock Desert: *Transaction, Geothermal Resources Council*, v. 38, p. 1041–1045.
- Harrison, W.E., Luza, K.V., Prater, M.L., and Cheung, P.K., 1983, Geothermal resource assessment in Oklahoma: Oklahoma Geological Survey Special Publication 83–1, 42 p.
- Henrikson, A., 2000, Heat flow determination from oil and gas wells in the Colorado Plateau and Basin and Range of Utah: Salt Lake City, University of Utah, M.S. thesis, 69 p.
- Henrikson, A., and Chapman, D.S., 2002, Terrestrial heat flow in Utah: Salt Lake City, University of Utah, unpublished report, 47 p.
- Hermanrud, C., Cao, S., and Lerche, I., 1990, Estimates of virgin rock temperature derived from BHT measurements—bias and error: *Geophysics*, v. 55, no. 7, p. 924–931.
- Horner, D.R., 1951, Pressure build-up in wells, in *3rd World Petroleum Congress*, The Hague, the Netherlands, May 28–June 6, 1951, *Proceedings: World Petroleum Congress*, p. 25–43.
- Howells, L., Longson, M.S., and Hunt, G.L., 1987, Base of moderately saline ground water in the Uinta Basin, Utah, with an introductory section describing the methods used in determining its position: Utah Department of Natural Resources Technical Publication 92, 59 p., 2 plates, scale 1:250,000. Also available as: U.S. Geological Survey Open-File Report 87-394.
- Kehle, R.O., Schoepel, R.J., and DeFord, R.K., 1970, The AAPG geothermal survey of North America: U.N. Symposium on the Development and Utilization of Geothermal Resources, Pisa, Italy, *Geothermics Special Issue 2*, p. 358–367.
- Keho, T.H., 1987, Heat flow in the Uinta Basin determined from bottom hole temperature (BHT) data: Salt Lake City, University of Utah, M.S. thesis, 99 p.
- Kutasov, I.M., and Eppelbaum, L.V., 2005, An improved Horner method for determination of formation temperature, in *World Geothermal Congress 2005*, Antalya, Turkey, April 24–29, 2005, *Proceedings: International Geothermal Association*, 8 p.
- Lachenbruch, A.H., and Brewer, M.C., 1959, Dissipa-



- tion of the temperature effect of drilling a well in Arctic Alaska: U.S. Geological Survey Bulletin 1083-C, p. 73–109.
- Luheshi, M.N., 1983, Estimation of formation temperature from borehole measurements: *Geophysical Journal*, Royal Astronomical Society, v. 74, p. 747–776.
- Lund, J.W., 2011, Development of Direct-Use Projects, *in* Thirty-Sixth Workshop on Geothermal Reservoir Engineering, Stanford, California, January 31–February 2, 2011, Proceedings: Stanford University, SGP-TR-191, 11 p.
- Morgan, P., and Scott, B., 2011, Bottom-hole temperatures data from the Piceance Basin, Colorado—indications for prospective sedimentary basin EGS resources: *Transactions, Geothermal Resources Council*, v. 35, p. 477–485.
- Morgan, P., and Scott, P., 2014, New geothermal-gradient maps for Colorado's sedimentary basins: *Transactions, Geothermal Resources Council*, v. 38, p. 155–162.
- Prensky, S., 1992, Temperature measurements in boreholes—an overview of engineering and scientific applications: *The Log Analyst*, v. 33, no. 3, p. 313–333.
- Shalev, E., Levitte, D., Gabay, R., and Zemach, E., 2008, Assessment of geothermal resources in Israel: Geological Survey of Israel Report GSI /29/ 2008, 26 p.
- Speece, M.A., Bowen, T.D., Folcik, J.L., and Pollack, H.N., 1985, Analysis of temperatures in sedimentary basins—the Michigan Basin: *Geophysics*, v. 50, p. 1218–1334.
- Steeple, D.W., and Stavnes, S.A., 1982, Assessment of geothermal resources of Kansas: U.S. Department of Energy Final Report DOE/ET/27204-T1-Vol. 1-Sect.1, 59 p.
- U.S. Bureau of Land Management, 2012, Greater Uinta Basin oil and gas cumulative impacts technical support document: U.S. Bureau of Land Management technical report, 27 p.
- Welhan, J., and Gwynn, M., 2014, High heat flow in the Idaho thrust belt—a hot sedimentary geothermal prospect: *Transactions, Geothermal Resources Council*, v. 38, p. 1055–1066.
- Welhan, J.A., Gwynn, M.L., Payne, S., McCurry, M.O., Plummer, M., and Wood, T., 2014, The Blackfoot volcanic field, Southeast Idaho—a hidden high-temperature geothermal resource in the Idaho thrust belt, *in* Thirty-Ninth Workshop on Geothermal Reservoir Engineering, Stanford, California, February 24–26, 2014, Proceedings: Stanford University, SGP-TR-202, 13 p.
- Willett, S.D., and Chapman, D.S., 1987, Analysis of temperatures and thermal processes in the Uinta Basin, *in* Beaumont, C., and Tankard, A.J., editors, *Sedimentary basins and basin-forming mechanisms*: Canadian Society of Petroleum Geologists Memoir No. 12, p. 227–261.
- Zhang, Y., Gable, C.W., Zyvoloski, G.A., and Walter, L.M., 2009, Hydrogeochemistry and gas compositions of the Uinta Basin—a regional-scale overview: *American Association of Petroleum Geologists Bulletin*, v. 93, no. 8, p. 1087–1118.
- Zschocke, A., 2005, Correction of non-equilibrated temperature logs and implications for geothermal investigations: *Journal of Geophysics and Engineering*, v. 2, p. 364–371.